Cleavage of Protein Kinase D After Acute Hypoinsulinemia Prevents Excessive Lipoprotein Lipase–Mediated Cardiac Triglyceride Accumulation

Min Suk Kim,[1] Fang Wang,[1] Prasanth Puthanveetil,[1] Girish Kewalramani,[1] Sheila Innis,[2] Lucy Marzban,[1] Susan F. Steinberg,[3] Travis D. Webber,[4] Timothy J. Kieffer,[4] Ashraf Abrahani,[1] and Brian Rodrigues[1]

OBJECTIVE—During hypoinsulinemia, when cardiac glucose utilization is impaired, the heart rapidly adapts to using more fatty acids. One means by which this is achieved is through lipoprotein lipase (LPL). We determined the mechanisms by which the heart regulates LPL after acute hypoinsulinemia.

RESEARCH DESIGN AND METHODS—We used two different doses of streptozocin (55 [D-55] and 100 [D-100] mg/kg) to induce moderate and severe hypoinsulinemia, respectively, in rats. Isolated cardiomyocytes were also used for transfection or silencing of protein kinase D (PKD) and caspase-3.

RESULTS—There was substantial increase in LPL in D-55 hearts, an effect that was absent in severely hypoinsulinemic D-100 animals. Measurement of PKD, a key element involved in increasing LPL, revealed that only D-100 hearts showed an increase in proteolysis of PKD, an effect that required activation of caspase-3 together with loss of 14-3-3ζ, a binding protein that protects enzymes against degradation. In vitro, phosphomimetic PKD colocalized with LPL in the trans-golgi. PKD, when mutated to prevent its cleavage by caspase-3 and silencing of caspase-3, was able to increase LPL activity. Using a caspase inhibitor (Z-DEVD) in D-100 animals, we effectively lowered caspase-3 activity, prevented PKD cleavage, and increased LPL vesicle formation and translocation to the vascular lumen. This increase in cardiac luminal LPL was associated with a striking accumulation of cardiac triglyceride in Z-DEVD–treated D-100 rats.

CONCLUSIONS—After severe hypoinsulinemia, activation of caspase-3 can restrict LPL translocation to the vascular lumen. When caspase-3 is inhibited, this compensatory response is lost, leading to lipid accumulation in the heart. *Diabetes* 58:2464–2475, 2009

Cardiac muscle has a high demand for energy and can use multiple substrates (1). Among these, glucose (~30%) and fatty acid (~70%) are the major sources from which the heart derives most of its energy (2). Fatty acid delivery and utilization by the heart involves *1*) release from adipose tissue and transport to the heart after complexing with albumin (3), *2*) provision through the breakdown of endogenous cardiac triglyceride (4), *3*) internalization of whole lipoproteins (5), and *4*) hydrolysis of circulating triglyceride-rich lipoproteins to fatty acids by lipoprotein lipase (LPL) positioned at the endothelial surface of the coronary lumen (6). The molar concentration of fatty acids bound to albumin is ~10-fold less than that of fatty acids in lipoprotein triglycerides, (7) and LPL-mediated hydrolysis of triglyceride-rich lipoproteins is suggested to be the principal source of fatty acids for cardiac utilization (8). Coronary endothelial cells do not synthesize LPL (9). In the heart, this enzyme is produced in cardiomyocytes and subsequently secreted onto heparan sulfate proteoglycan (HSPG) binding sites on the myocyte cell surface (10). From here, LPL is transported onto comparable binding sites on the luminal surface of endothelial cells (11). At the lumen, LPL actively metabolizes the triglyceride core of lipoproteins; the released fatty acids are then transported into the heart.

The earliest change that occurs in the type 1 diabetic heart is altered energy metabolism where in the presence of lower glucose utilization, the heart switches to using more fatty acids for energy supply (12). One means by which this is possible is through an increase in LPL at the coronary lumen. Using retrograde perfusion of the heart with heparin to displace vascular LPL, we found elevated LPL following diabetes (13–15). We determined that the increased enzyme is *1*) not the result of increased gene expression (13), *2*) unrelated to an increase in the number of endothelial HSPG binding sites (13), *3*) associated with an acute reduction in insulin (within 60 min) (16), and *4*) functionally relevant and capable of hydrolyzing lipoprotein triglycerides (17). More recently, we examined the contributions of the cardiomyocyte and endothelial cell in enabling this increased enzyme at the vascular lumen. Within the myocyte, LPL vesicle fission was regulated by protein kinase D (PKD) (18), whereas recruitment of LPL to the cardiomyocyte surface was controlled by stress kinases like AMP-activated protein kinase (AMPK) (19) and p38 mitogen-activated protein kinase (MAPK) that allowed for provision of an actin network that facilitated

The costs of publication of this article were defrayed in part by the payment of page charges. This article must therefore be hereby marked "advertisement" in accordance with 18 U.S.C. Section 1734 solely to indicate this fact.

LPL movement (20). Translocation of LPL from the cardiomyocyte surface to the apical side of endothelial cells is then dependent on the ability of the endothelium to release heparanase (21,22), which enables myocyte HSPG cleavage and transfer of LPL toward the coronary lumen.

Selective β-cell death and an ensuing diabetic state can be produced after a single intravenous dose of streptozotocin (STZ) (23). In Wistar rats, a dose-dependent increase in severity of diabetes is produced by 25–100 mg/kg STZ (24). After injection of 55 mg/kg (D-55), stable hyperglycemia develops within 24–48 h in concert with a ~50% reduction in plasma insulin (16,24). Although these animals were insulin deficient, they did not require insulin supplementation for survival and did not develop ketoacidosis. In the absence of any changes in plasma fatty acids and triglycerides, these animals demonstrated an increase in coronary vascular LPL (13–15). Rats administered 100 mg/kg STZ (D-100) demonstrated intense β-cell necrosis, loss of 98% pancreatic insulin stores, and severely reduced plasma insulin (16). Compared to D-55 diabetic rats, these D-100 animals show a remarkable elevation of plasma fatty acids and triglycerides. Importantly, LPL activity decreases (14,25) in D-100 hearts, suggesting a potential mechanism to restrain LPL-derived fatty acids when the supply of this substrate from other reservoirs is in surplus. The objective of the present study was to determine the mechanisms by which the hypoinsulinemic heart limits its LPL-derived fatty acids under conditions of hyperlipidemia. Our data demonstrate that caspase-3 activation, by cleaving PKD, attempts to restrict the hydrolysis of circulating triglyceride by LPL to limit fatty acid provision and cardiac triglyceride overload. Thus, although caspase-3 inhibition could be protective in reducing cell death, its augmentation of LPL may induce profound cardiac triglyceride accumulation.

RESEARCH DESIGN AND METHODS

An expanded version of the RESEARCH DESIGN AND METHODS has been described in the online appendix that is available at http://diabetes.diabetesjournals.org/cgi/content/full/db09-0681/DC1. In this supplement, we have explained our animal model of hypoinsulinemia, perfusion of isolated hearts, isolation of cardiomyocytes, assay for LPL activity, adenoviral transfection of cardiac cells, Western blotting, immunoprecipitation, immunofluorescence, measurement of cardiac triglyceride, heart fractionation and estimation of lipid droplet protein, electron microscopy, plasma membrane CD36 determination, palmitate oxidation, and separation of golgi.

RESULTS

Severity of diabetes determines the magnitude of LPL at the coronary lumen. By exploiting two different doses of STZ, we induced moderate (55 mg/kg) and severe (100 mg/kg) hypoinsulinemia. Although both groups were equally hyperglycemic (Fig. 1A, inset), D-100 rats showed a more profound loss of circulating insulin (Fig. 1A). During hypoinsulinemia, excessive lipolysis and loss of adipose tissue mass results in an increase in both plasma fatty acids and triglycerides (24). Indeed, both plasma fatty acids (Fig. 1B) and triglycerides (Fig. 1B, inset) levels were elevated in D-100 animals. Interestingly, measurement of these parameters in D-55 showed no significant differences when compared to control subjects (Fig. 1B). During hypoinsulinemia with its attendant loss of glucose utilization, LPL activity increases at the vascular lumen (13). Compared to control hearts, there was substantial increase in heparin-releasable LPL activity in D-55 animals (Fig. 1C), with most of the enzyme located at the vascular

lumen as shown using immunofluorescence (Fig. 1E). Contrary to the results obtained with D-55 rats, heparin-releasable LPL activity (Fig. 1C) and LPL immunofluorescence (Fig. 1E) in severely hypoinsulinemic D-100 animals were unchanged when compared to control subjects. Both hypoinsulinemic groups showed no significant change in cardiac LPL gene expression (Fig. 1D).

Caspase-3 produces proteolysis of cardiac PKD. Recently, we have reported that phosphorylation of PKD is a key element to increase cardiac LPL after hyperglycemia (D-55) by regulating fission of vesicles from golgi membranes (18). In the present study, measurement of PKD revealed that only D-100 hearts showed a decrease in full-length PKD (Fig. 2A, inset), with a corresponding robust increase in the cleaved form (Fig. 2A), that increases its activity (26) but limits its golgi-binding capability (27). In U-937 leukemic monocyte lymphoma cells, caspase-3 has been suggested to control PKD by cleaving its cysteine-rich domain (26), which is necessary for binding to trans-golgi (27). Measurement of caspase-3 in D-100 rat hearts demonstrated an increase in its activity (Fig. 2B). This increase was modest; PAC-1, a procaspase-3 activator, increased caspase-3 activity twofold higher than D-100. Transferase-mediated dUTP nick-end labeling (TUNEL) and DAPI nuclear staining were used to assess cell apoptosis. Hearts from D-100 animals exhibited a higher number of apoptotic cells. However, the overall percentage of these cells was very low (~0.01%) (data not shown). Given the effect of caspase-3 to cleave PKD, purified glutathione S-transferase (GST)-PKD was incubated with active caspase-3 enzyme. As predicted, GST-PKD was rapidly cleaved by caspase-3 (Fig. 2C). Replicating this experiment using PKD isolated from control hearts also showed cleavage of PKD by caspase-3. However, caspase-3 proteolysis of GST-PKD was faster than its cleavage of isolated PKD from control hearts (Fig. 2D). Interestingly, although D-55 hearts also showed an increase in caspase-3 activity (Fig. 2B), this was not associated with cleaved PKD (Fig. 2A), suggesting that in D-55 hearts some protein is preventing PKD cleavage. Proteins 14–3-3 are binding proteins known to interact with a number of enzymes protecting them against proteolytic degradation (28), and diabetes is known to decrease the gene and protein expression of 14–3-3ζ (29). Measurement of 14–3-3ζ showed a decrease in its mRNA (Fig. 2E) and protein (Fig. 2E, inset), only in D-100 hearts. In addition, severe hypoinsulinemia also resulted in a decreased attachment of PKD to 14–3-3ζ (Fig. 2F). Silencing of 14–3-3ζ in cardiomyocytes had no influence on PKD expression (Fig. 2G, inset). Nevertheless, in these cells, exposure to caspase-3 accelerated PKD cleavage (Fig. 2G, boxed inset). Our data suggest that both activation of caspase-3 together with loss of 14-3-3ζ are required for cleavage of PKD after severe hypoinsulinemia.

Manipulating PKD in isolated cardiomyocytes is sufficient to regulate heparin-releasable LPL. In cardiomyocytes, phosphomimetic (PKD-S744E/S748E) and kinase-dead mutants of PKD were overexpressed by adenoviral vectors to establish the relationship between PKD and LPL. First, we validated successful transduction using Western blotting (Fig. 3A). Both PKD-S744E/S748E and kinase-dead mutants increased total PKD expression (Fig. 3A, inset); only the phosphomimetic mutant demonstrated higher Ser[916] phosphorylation, which is related to its catalytic activity (30). The S744/S748 phosphorylation site has been shown to have a critical role in recruiting PKD
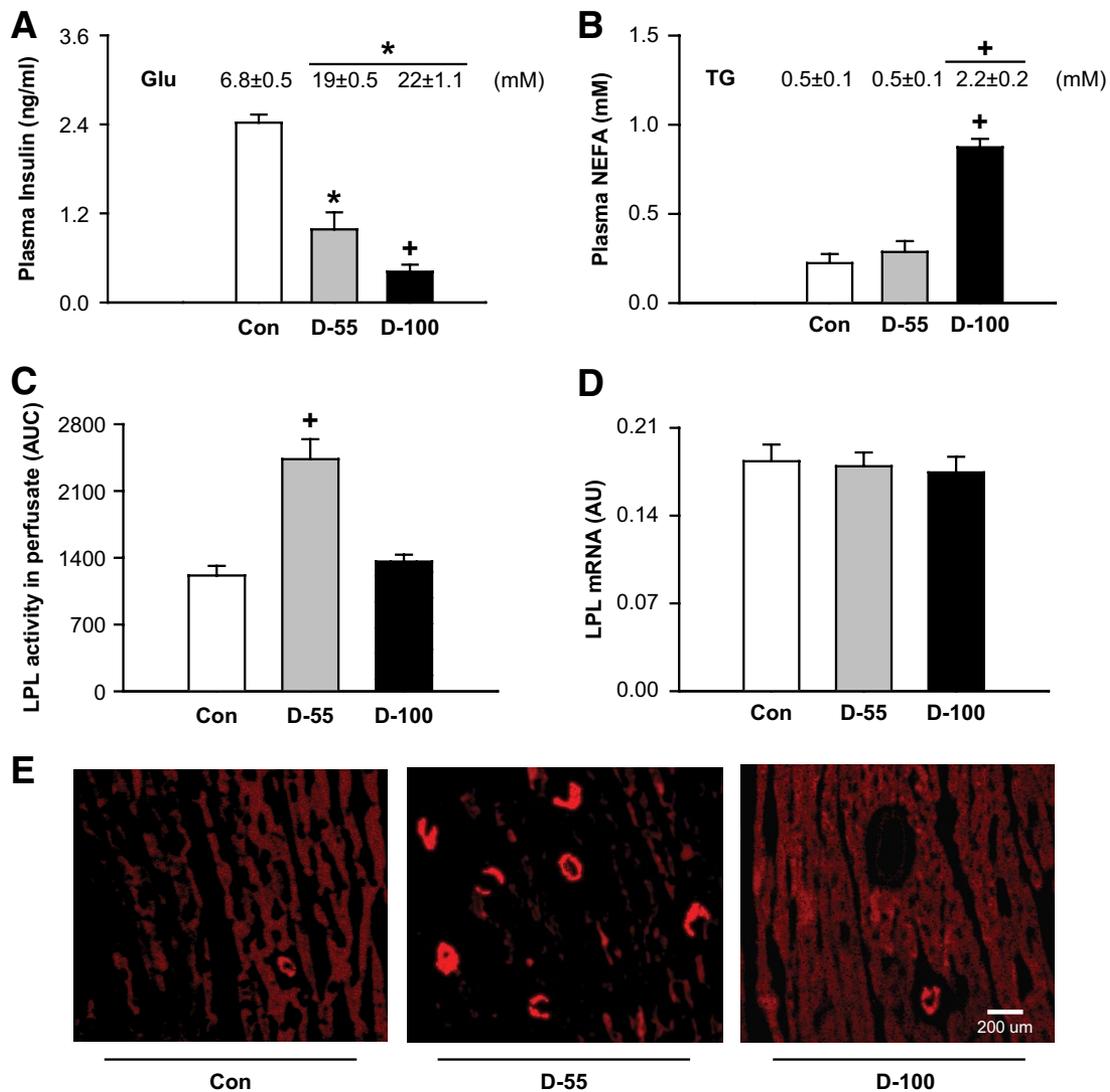
FIG. 1. Moderate and severe hypoinsulinemia have dissimilar effects on cardiac LPL. Animals were treated with two different doses of STZ (55 [D-55] and 100 [D-100] mg/kg) and kept for 4 days. Fed blood samples were obtained from the tail vein and glucose (Glu) determined using a glucometer (A, $inset$). Plasma was assayed for insulin (A), triglyceride (B, $inset$), and nonesterified fatty acids (NEFA, B) using diagnostic kits. Hearts were isolated and perfused in the nonrecirculating retrograde mode. The coronary luminal LPL released with heparin (5 units/ml) was collected and LPL activity was assayed using radiolabeled triolein. LPL activity was determined as nmol · h^{-1} · ml^{-1}. The results are expressed as area under curve of enzyme released over 5 min (C). LPL mRNA was measured using real-time PCR (D). LPL was visualized by immunofluoresence (E). Bar = 200 μm. Results are the means ± SE of 3–5 rats in each group. *Significantly different from control subjects; +significantly different from all other groups, $P < 0.05$. AU, arbitrary units; AUC, area under curve; TG, triglyceride. (A high-quality color digital representation of this figure is available in the online issue.)

to the trans-golgi (27). Simply increasing the expression of the phosphomimetic and kinase-dead mutants augmented their association with the trans-golgi (supplemental Fig. IA). However, PKD-S744E/S748E also increased the colocalization of LPL to the trans-golgi (Fig. 3C), with a striking increase in heparin-releasable LPL activity (Fig. 3B).

Using a different strategy, cardiomyocytes were transfected with PKD-D378A point mutated to prevent caspase-3–mediated proteolysis (26). Successful transfection of PKD wild type and PKD-D378A is demonstrated in supplemental Fig. 1B. Although PKD wild type and PKD-D378A themselves elevated PKD phosphorylation at Ser^{916}, phosphorylation of Ser$^{744/748}$ (supplemental Fig. IB) and heparin-releasable LPL activity (supplemental Fig. IC) remained unchanged compared to enhanced green fluorescent protein (EGFP). Bryostatin-1 is a potent activator of PKD (31). Control cardiomyocytes treated

with bryostatin-1 increased phosphorylation (both S744/S748 and Ser^{916}) of PKD and heparin-releasable LPL activity (Fig. 3D, $inset$). In wild-type and D378A cardiomyocytes, bryostatin-1 was not only capable of further increasing Ser^{916} phosphorylation but also Ser$^{744/748}$ phosphorylation (supplemental Fig. IB). In these myocytes, bryostatin-1 also elicited a robust increase in heparin-releasable LPL activity (supplemental Fig. IC). Pretreating EGFP and wild-type cells with PAC-1 followed by bryostatin-1 induced significant cleavage of PKD, an effect that was not apparent in PKD-D378A cardiomyocytes (Fig. 3D). More importantly, caspase-3 activation in D378A did not decrease LPL activity as seen in EGFP and wild type (Fig. 3E). It should be noted that in this experiment, using nondiabetic myocytes 14-3-3ζ was unable to protect PKD from cleavage by PAC-1, which elicited a more robust increase in caspase-3 compared to D-100. Overall, these data suggest that LPL transport to the
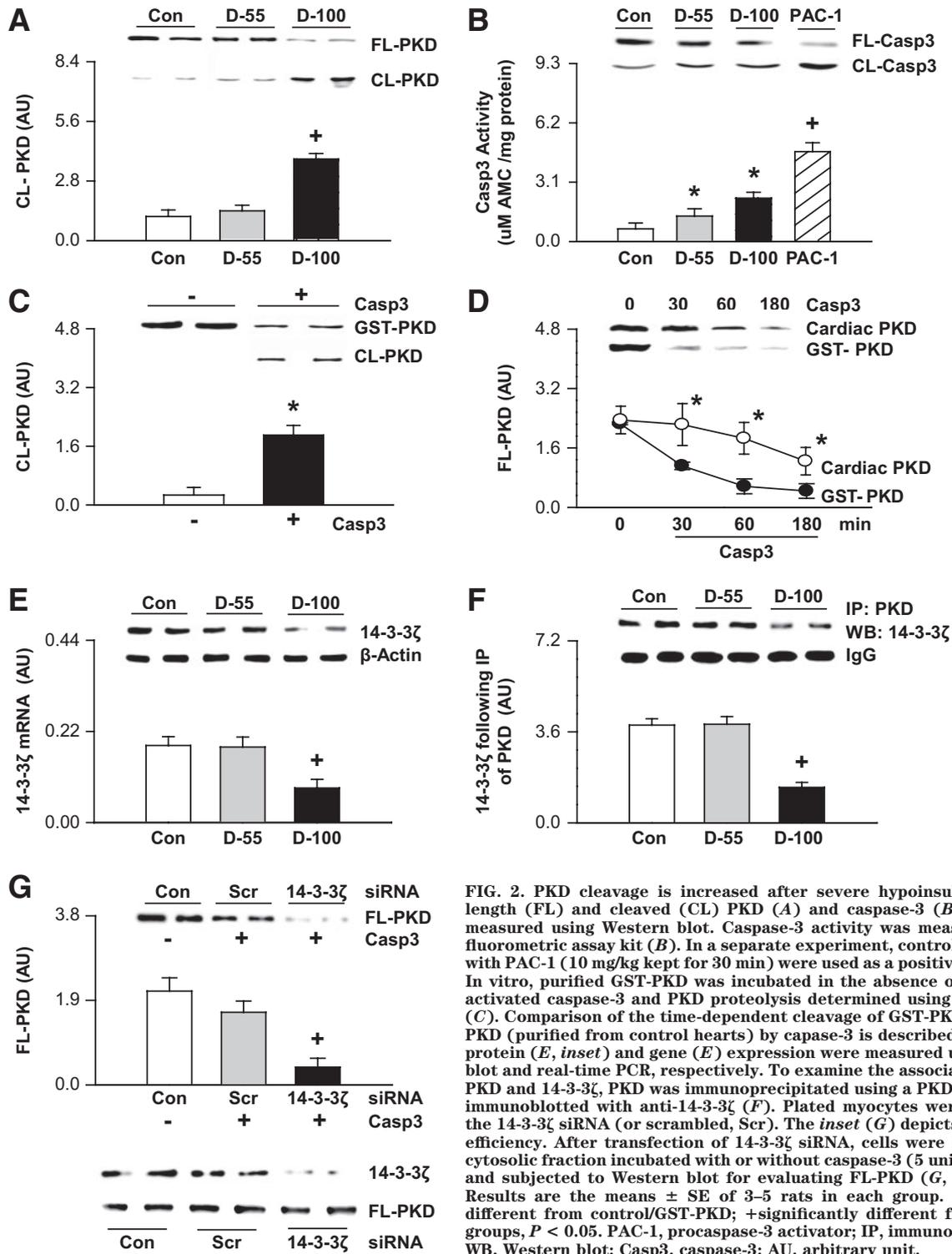
FIG. 2. PKD cleavage is increased after severe hypoinsulinemia. Full-length (FL) and cleaved (CL) PKD (*A*) and caspase-3 (*B*, *inset*) were measured using Western blot. Caspase-3 activity was measured using a fluorometric assay kit (*B*). In a separate experiment, control rats injected with PAC-1 (10 mg/kg kept for 30 min) were used as a positive control (*B*). In vitro, purified GST-PKD was incubated in the absence or presence of activated caspase-3 and PKD proteolysis determined using Western blot (*C*). Comparison of the time-dependent cleavage of GST-PKD and cardiac PKD (purified from control hearts) by capase-3 is described in *D*. 14-3-3ζ protein (*E*, *inset*) and gene (*E*) expression were measured using Western blot and real-time PCR, respectively. To examine the association between PKD and 14-3-3ζ, PKD was immunoprecipitated using a PKD antibody and immunoblotted with anti-14-3-3ζ (*F*). Plated myocytes were exposed to the 14-3-3ζ siRNA (or scrambled, Scr). The *inset* (*G*) depicts transfection efficiency. After transfection of 14-3-3ζ siRNA, cells were lysed and the cytosolic fraction incubated with or without caspase-3 (5 units for 30 min) and subjected to Western blot for evaluating FL-PKD (*G*, *boxed inset*). Results are the means ± SE of 3–5 rats in each group. *Significantly different from control/GST-PKD; +significantly different from all other groups, *P* < 0.05. PAC-1, procaspase-3 activator; IP, immunoprecipitation; WB, Western blot; Casp3, caspase-3; AU, arbitrary unit.

cell surface is dependent on PKD phosphorylation at S744/S748 rather than PKD's intrinsic activity and that cleavage of PKD by caspase-3 is sufficient to prevent PKD-mediated increase in LPL activity.

Silencing of caspase-3 prevents PKD proteolysis and increases cardiac LPL activity. We used siRNA to silence caspase-3 in isolated cardiomyocytes. We first validated successful caspase-3 inhibition using Western blotting (Fig. 4*A*, *inset*). In myocytes in which caspase-3 was silenced, PAC-1 was unable to increase caspase-3 activity (Fig. 4*A*) or to increase PKD cleavage (Fig. 4*B*).

Furthermore, in myocytes in which caspase-3 was silenced, the PAC-1–induced decrease in LPL activity was prevented (Fig. 4*C*).

Caspase-3 restricts PKD-mediated LPL vesicle formation. PKD, by associating with vesicle-associated membrane protein (VAMP, one of v-SNAREs), is known to trigger vesicular movement (32). To further elucidate the interactions between caspase-3, PKD, and LPL, purified golgi were incubated in the presence or absence of GST-PKD and caspase-3 and vesicle formation determined using antibodies against VAMP. As predicted, VAMP-asso-
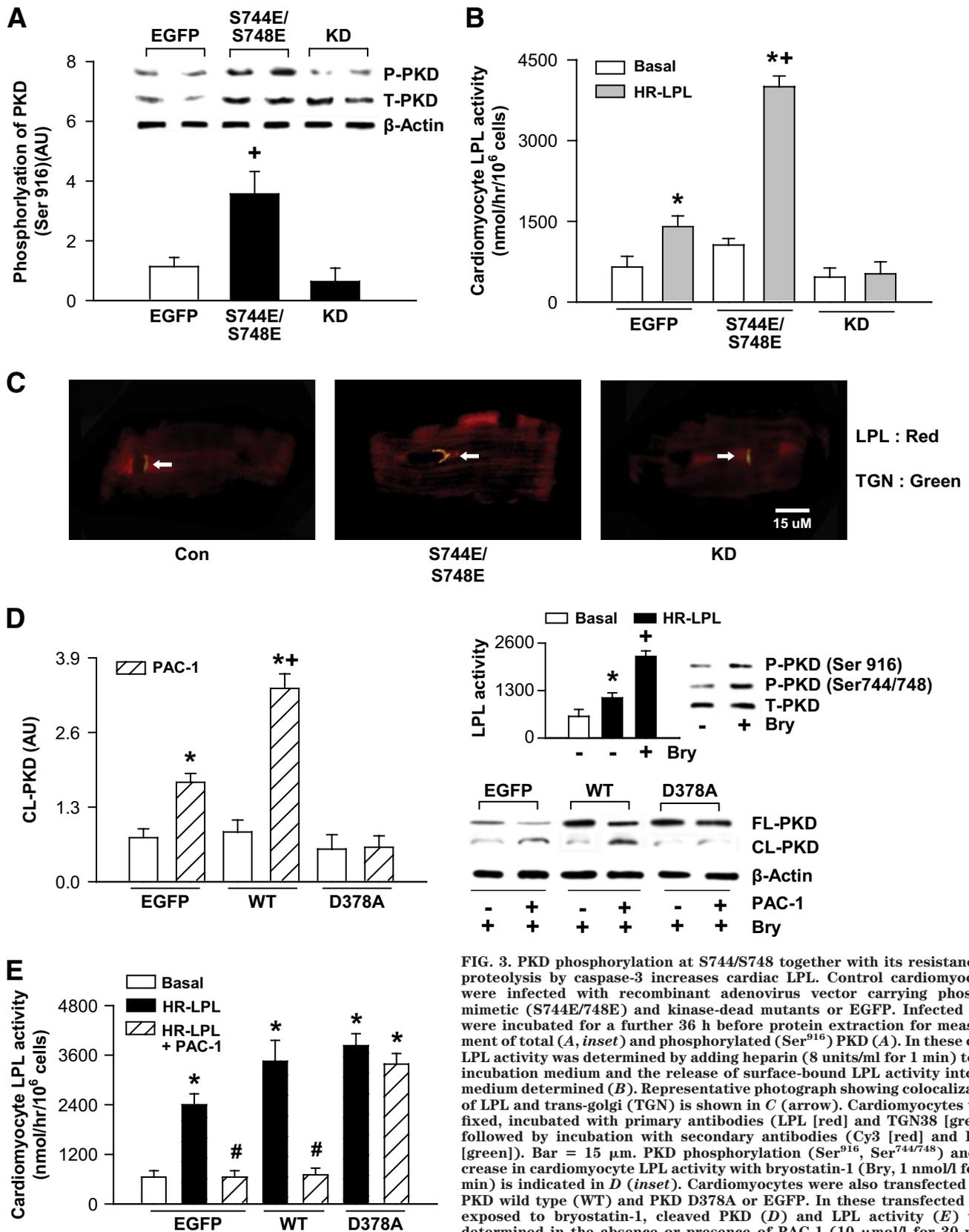
FIG. 3. PKD phosphorylation at S744/S748 together with its resistance to proteolysis by caspase-3 increases cardiac LPL. Control cardiomyocytes were infected with recombinant adenovirus vector carrying phosphomimetic (S744E/748E) and kinase-dead mutants or EGFP. Infected cells were incubated for a further 36 h before protein extraction for measurement of total (*A, inset*) and phosphorylated (Ser[916]) PKD (*A*). In these cells, LPL activity was determined by adding heparin (8 units/ml for 1 min) to the incubation medium and the release of surface-bound LPL activity into the medium determined (*B*). Representative photograph showing colocalization of LPL and trans-golgi (TGN) is shown in *C* (arrow). Cardiomyocytes were fixed, incubated with primary antibodies (LPL [red] and TGN38 [green]) followed by incubation with secondary antibodies (Cy3 [red] and FITC [green]). Bar = 15 μm. PKD phosphorylation (Ser[916], Ser[744/748]) and increase in cardiomyocyte LPL activity with bryostatin-1 (Bry, 1 nmol/l for 30 min) is indicated in *D* (*inset*). Cardiomyocytes were also transfected with PKD wild type (WT) and PKD D378A or EGFP. In these transfected cells exposed to bryostatin-1, cleaved PKD (*D*) and LPL activity (*E*) were determined in the absence or presence of PAC-1 (10 μmol/l for 30 min). Results are the means ± SE of 3–5 cardiomyocyte preparations from different animals. *Significantly different from control subjects; +significantly different from all other groups; #significantly different from heparin releasable, $P < 0.05$. Casp3, caspase-3; HR, heparin-releasable; P, phosphorylated; T, total. (A high-quality color digital representation of this figure is available in the online issue.)
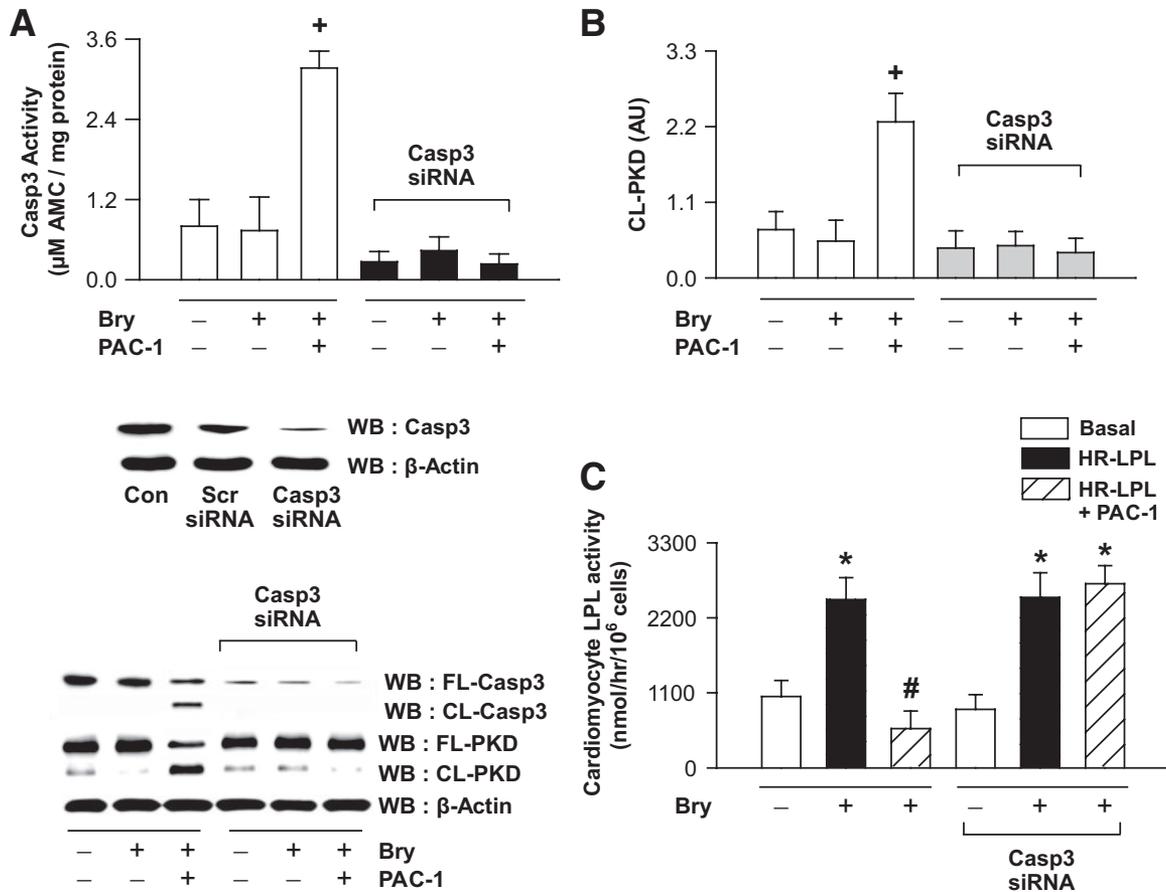
FIG. 4. Impeding PKD proteolysis by silencing caspase-3 substantially increases cardiac LPL activity. Plated myocytes were exposed to the caspase-3 siRNA (or scrambled, Scr). The *inset* (*A*) depicts transfection efficiency. After transfection of caspase-3 siRNA, cells were treated with or without PAC-1 (10 μmol/l for 30 min), lysed, and subjected to Western blot for evaluating full-length (FL) and cleaved (CL) caspase-3 and PKD (*A* and *B*). Caspase-3 activity was measured using a fluorometric assay kit (*A*). In these cells, LPL activity was determined by adding heparin to the incubation medium and the release of surface-bound LPL activity into the medium determined (*C*). Bryostatin-1 (Bry, 1 nmol/l for 30 min) was used to activate PKD. Results are the means ± SE of 3–5 cardiomyocyte preparations from different animals. *Significantly different from control subjects; +significantly different from all other groups; #significantly different from heparin releasable, $P < 0.05$. AU, arbitrary unit; Casp3, caspase-3; WB, Western blot.

ciated vesicle formation significantly increased on incubation with GST-PKD; the GST-PKD–induced vesicles contained high levels of LPL (Fig. 5*A* and *B*). These effects of PKD on VAMP-associated vesicle formation and LPL content were impeded by caspase-3 (Fig. 5*A* and *B*). We applied a similar approach in vivo, using Z-DEVD to inhibit caspase-3 in D-100 hearts. Interestingly, when the cytosolic fraction from Z-DEVD–treated D-100 hearts was incubated with isolated golgi, VAMP-associated vesicular formation together with LPL vesicle content increased significantly (Fig. 5*C* and *D*).

Inhibiting caspase-3 in D-100 rats increases LPL at the vascular lumen. Given the strong relationship between caspase-3 and LPL, D-100 rats were treated with the caspase-3 inhibitor Z-DEVD and LPL activity determined. Z-DEVD was very effective in preventing caspase-3 cleavage and its subsequent activation (Fig. 6*A*). More importantly, this caspase-3 inhibitor prevented the cleavage of PKD that is seen in D-100 hearts (Fig. 6*B*). This effect on PKD in Z-DEVD–treated D-100 hearts increased the appearance of LPL at the vascular lumen (Fig. 6*D*), in addition to augmenting heparin-releasable LPL activity (Fig. 6*C*) to levels observed in D-55 hearts. Z-DEVD had no influence on total LPL expression, which remained ~20% lower than that in control subjects (Fig. 6*E*). In addition, Z-DEVD had no further influence in increasing vascular LPL in D-55

hearts (data not shown). In summary, activation of caspase-3 in D-100 hearts restrains the transfer of LPL to the coronary lumen by affecting proteolysis of PKD.

Caspase-3 inhibition in D-100 promotes excessive cardiac triglyceride accumulation. Interestingly, the augmented amount of LPL in Z-DEVD–treated D-100 rats corresponded to an increased clearance of circulating triglyceride (Fig. 7*A*), without affecting plasma fatty acids (Fig. 7*B*). In these animals, unlike the drop in plasma triglyceride, there was a striking accumulation of cardiac triglyceride, which was almost twofold higher than that in the untreated D-100 animals (Fig. 7*C* and *D*). Sucrose fractionation and subjection of the different fractions to Western blotting for OXPAT or determination of triglyceride revealed that in D-100, the fractions (top) that had highest amount of triglycerides were associated with OXPAT (supplemental Fig. 2); caspase inhibition in D-100 induced a further increase of OXPAT in these fractions (supplemental Fig. 2). Hearts from D-100 animals demonstrated an approximately twofold increase in CD36 protein (Fig. 7*E*). Treatment of these animals with Z-DEVD did not initiate a further increase in plasma membrane CD36 (Fig. 7*E*). Cardiac palmitate oxidation in D-100 rats treated and untreated with Z-DEVD remained high (Fig. 7*F*).
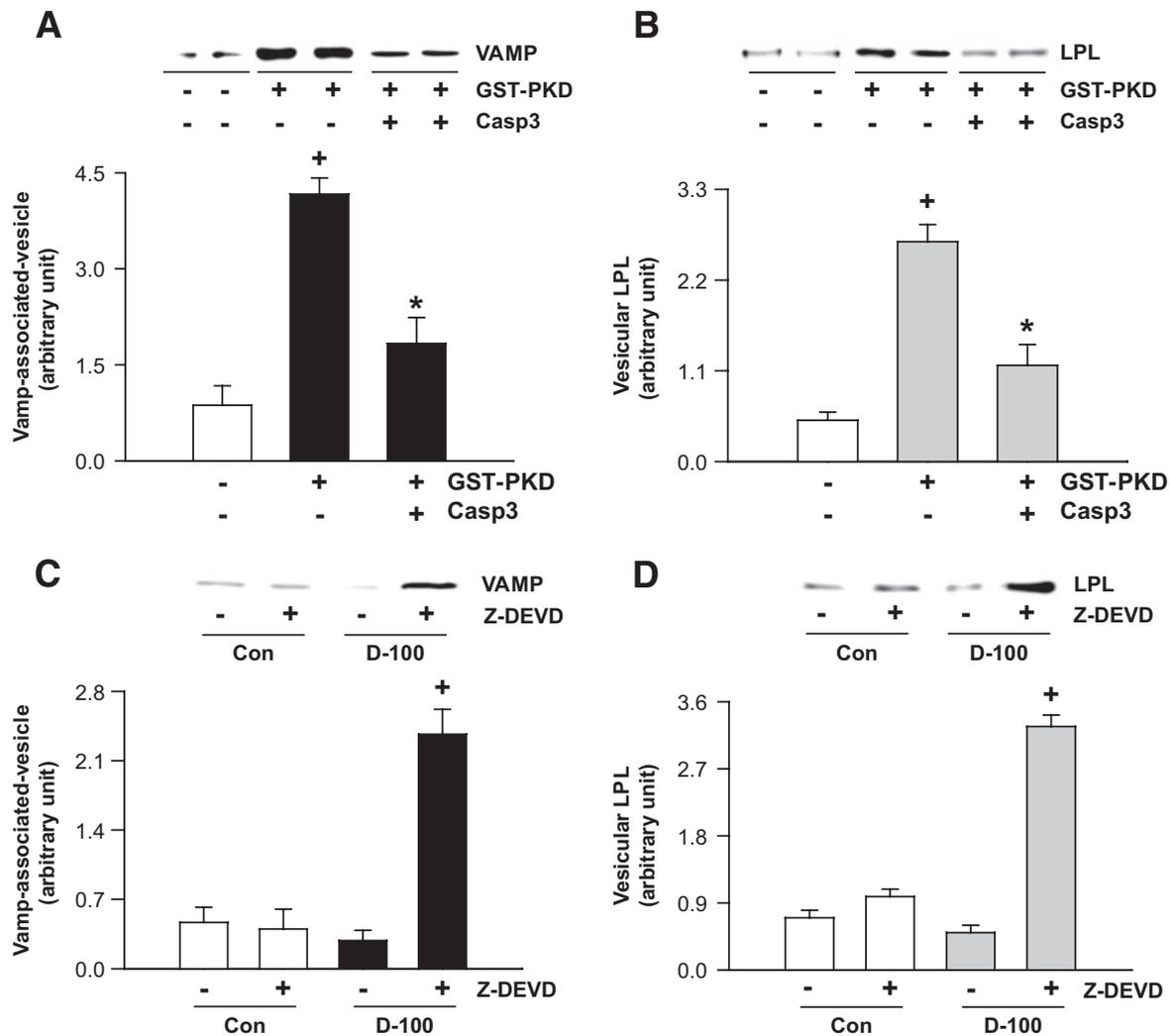
FIG. 5. Full-length PKD is essential for LPL vesicle formation from golgi. Rat heart homogenate was overlaid on sucrose solutions and the gradients centrifuged for 2 h. A golgi fraction was isolated from the sucrose interphase and mixed with GST-PKD (5 μg) alone or together with caspase-3 (Casp3) (5 units) (*A* and *B*). Isolated golgi were also incubated with cardiac cytosol (0.2 mg) isolated from control and D-100 hearts, treated or not treated with Z-DEVD (*C* and *D*). All samples were ultra centrifuged for isolation of vesicles, which were then subjected to Western blot for evaluating VAMP and LPL. Results are the means ± SE of 3–5 experiments in each group. *Significantly different from control subjects; +significantly different from all other groups, $P < 0.05$.

DISCUSSION

During diabetes, when cardiac glucose uptake, glycolysis, and pyruvate oxidation are impaired, the heart rapidly adapts to using a greater amount of fatty acids for ATP generation, allowing it to maintain its function (33). This change occurs not only as a consequence of increased exogenous fatty acids (because of release of fatty acids from adipose tissue and hydrolysis of triglyceride-rich lipoproteins by LPL) and endogenous fatty acids (hormone-sensitive lipase hydrolysis of intracellular stored triglycerides) supply but also through an intrinsic adaptation or maladaptation to elevated fatty acids that includes an augmented fatty acid oxidation and expression of genes that control utilization of this substrate (33). To avoid oversupply of this potentially lethal substrate, the heart can exquisitely regulate its LPL content at the vascular lumen. Thus, following moderate acute STZ diabetes (that resembles a poorly controlled type 1 diabetes patient), when circulating fatty acids and triglycerides have yet to increase, significantly elevated luminal LPL protein and activity is observed (14). Given that vascular endothelial LPL is acquired from the cardiomyocyte, we previously

examined the mechanisms by which diabetes increases cardiomyocyte cell surface LPL, a reservoir that can rapidly augment coronary luminal LPL when the need for fatty acids is intensified. In the myocyte, we reported that recruitment of LPL to the cell surface was controlled by PKD (that regulated LPL vesicle fission) (18), whereas stress kinases like AMPK and p38 MAPK allowed for actin cytoskeleton polymerization, providing the cardiomyocyte with an infrastructure to facilitate LPL movement (20). In the present study, our data demonstrate that after severe hypoinsulinemia (with its attendant elevation of plasma fatty acids and triglycerides), caspase-3 activation, by cleaving PKD, restricts amplification of LPL, thereby limiting fatty acid provision and overwhelming cardiac triglyceride accumulation.

The cytosolic serine-threonine kinase, PKC-μ, also known as PKD, regulates vesicular fission from the trans-golgi network, allowing cargo proteins to be delivered to the plasma membrane (27). Within PKD, a cysteine-rich domain has been shown to have a critical role in recruiting and binding PKD to the trans-golgi (27). We have recently reported that PKD is a key modulator of LPL vesicular
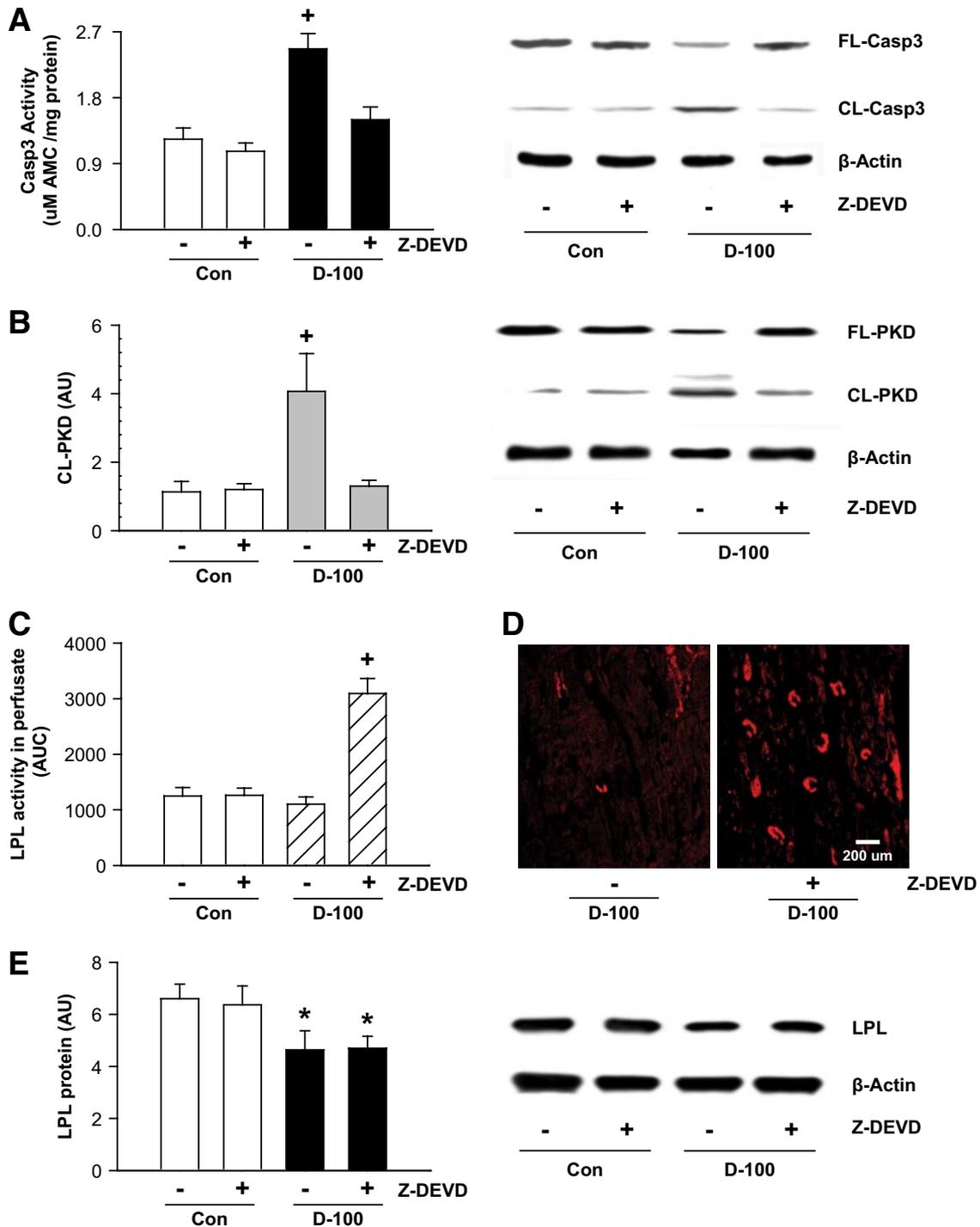
FIG. 6. Activation of caspase-3 in D-100 limits vascular lumen increase in LPL. Animals were treated with STZ (100 mg/kg, i.v.), and kept for 4 days. After 1 day of STZ, some control and D-100 rats were treated twice daily with Z-DEVD (3.2 mg/kg, i.p.) for 3 days. Cardiac caspase-3 activity was measured using a fluorometric assay kit (A). Full-length (FL) and cleaved (CL) caspase-3 (A) and PKD (B) in the different groups were measured using Western blot. Hearts were also isolated and perfused in the nonrecirculating retrograde mode. The coronary luminal LPL released with heparin (5 units/ml) was assayed using radiolabeled triolein. The results are expressed as area under curve (AUC) of enzyme released over 5 min (C). LPL was visualized by immunofluoresence (D). Bar = 200 μm. The level of LPL protein was measured using Western blot (E). Results are the means ± SE of 3–5 rats in each group. *Significantly different from control subjects; +significantly different from all other groups, $P < 0.05$. AU, arbitrary unit; Casp3, caspase-3. (A high-quality color digital representation of this figure is available in the online issue.)

trafficking within cardiomyocytes and is related not only to binding of PKD to the golgi (18) but also to phosphorylation of Ser$^{744/748}$ in its catalytic domain. In D-55 animals, PKD phosphorylation was strongly correlated to an increase in LPL on the luminal surface of the capillary endothelium. Given the observation that in hearts from D-100 animals LPL activity remained unchanged after 4

days or decreased after 1 week (14,25), we hypothesized that a signal deficiency for LPL translocation exists within these hearts. Interestingly, measurement of PKD revealed that only D-100 hearts showed a decrease in full-length PKD, with a corresponding robust increase in the cleaved form. Our data suggest that following severe hypoinsulinemia, proteolysis of PKD may be an impor-
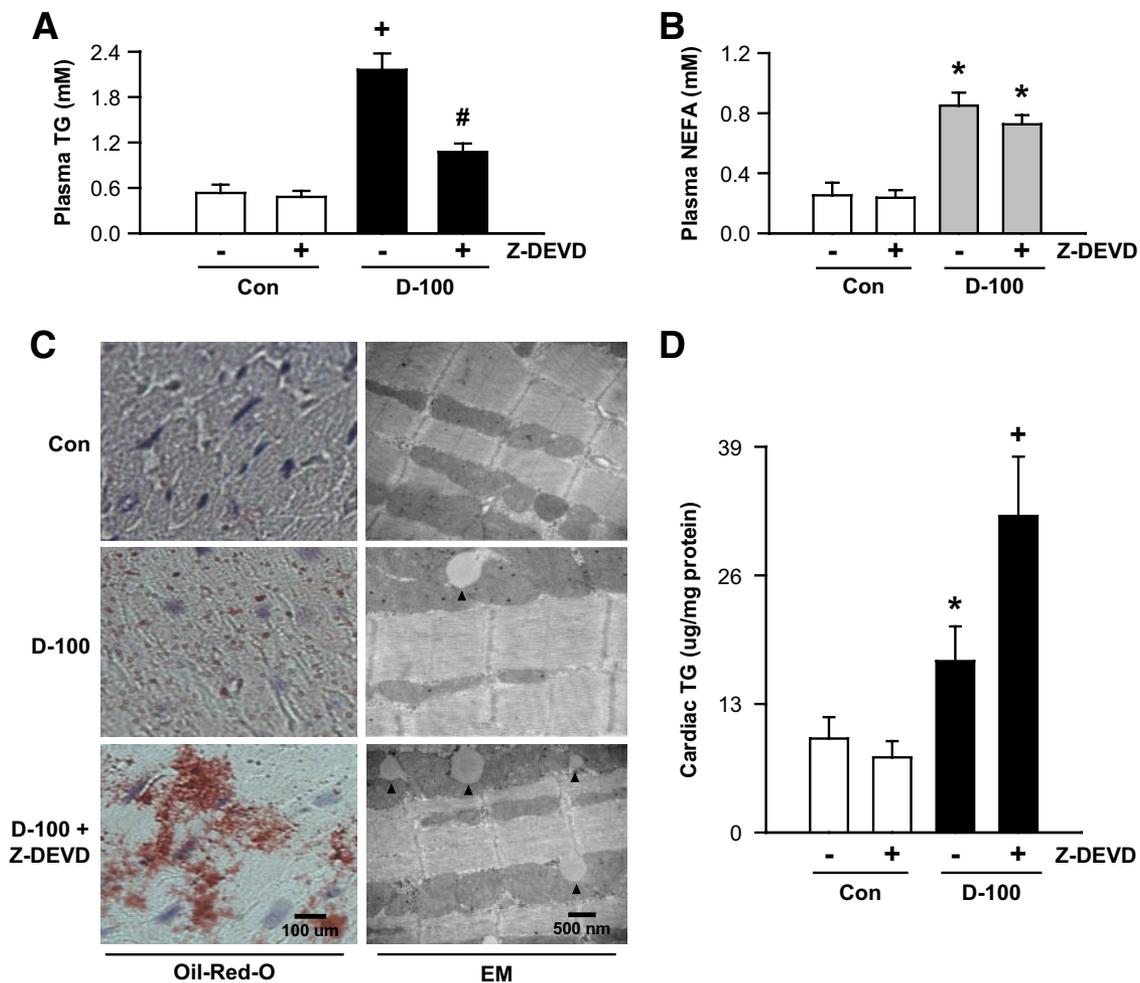
FIG. 7. Inhibition of caspase-3 facilitates a striking increase in triglyceride accumulation in D-100 hearts. Plasma collected at termination was evaluated for triglyceride (*A*) and NEFA (*B*) using diagnostic kits. Oil Red O staining of representative cardiac sections showing lipid accumulation is described in *C* (*left panel*). Bar = 100 μm. Representative electron micrograph of hearts from different groups is depicted in *C* (*right panel*). Bar = 500 nm. Black arrow head, lipid-like vacuoles. Cardiac triglyceride was extracted with organic solvent and determined using high-performance liquid chromatography (*D*). Plasma membranes were isolated and used for identification of CD36 (*E*). Palmitate oxidation in myocytes isolated from the different groups was assessed by measuring $^{14}CO_2$ (*F*). Results are the means ± SE of 3–5 rats in each group. *Significantly different from control subjects; +significantly different from all other groups; #significantly different from untreated D-100, $P <$ 0.05. A graphic representation of caspase-3 control of cardiac metabolism is described in *G*. After severe hypoinsulinemia, a decrease in full-length PKD requires both activation of caspase-3 together with loss of the binding protein 14-3-3ζ. Proteolysis of PKD is unable to transfer cardiac LPL to the vascular lumen. The caspase inhibitor, Z-DEVD, effectively lowers caspase-3 activity in D-100 hearts, prevents PKD cleavage, and increases LPL vesicle formation and translocation to the coronary lumen. This increase in luminal LPL is associated with a decline in circulating triglyceride but a striking cardiac triglyceride accumulation. AU, arbitrary unit; TG, triglyceride; Casp3, caspase-3. (A high-quality color digital representation of this figure is available in the online issue.)

tant event to limit an increase in LPL activity at the vascular lumen.

In U-937 cells, caspase-3 has been suggested to control PKD by cleaving its cysteine-rich domain (26). Given the relationship between caspase-3 and PKD, we measured caspase-3 and determined that both D-55 and D-100 hearts demonstrated an increase in its activity, likely mediated by reactive oxygen species (34). It should be noted that the observed increase of caspase-3 in these hearts did not reach the upper limit seen with PAC-1, the caspase-3 activator that induces apoptosis (programmed cell death). Thus, although caspase-3 plays a key role in apoptosis (35) in the acute hypoinsulinemic heart, caspase-3 may also have a nonapoptotic function. Other studies have also suggested that caspase-3 has a regulatory function in cell proliferation, differentiation, and shaping (36). This secondary function of caspase-3 in D-100 hearts included cleavage of PKD, an observation that was absent after moderate hypoinsulinemia, even though these hearts showed

an increase in caspase-3 activity. Given that *1*) measurement of 14-3-3ζ showed a decrease in its mRNA and protein only in D-100 hearts, *2*) caspase-3's proteolysis of cardiac PKD was slower than its cleavage of GST-PKD, and *3*) silencing of 14-3-3ζ in cardiomyocyte accelerated PKD cleavage on exposure of these cells to caspase-3, our data suggest that this 14-3-3ζ binding protein protects PKD against proteolytic degradation by caspase-3 in D-55. Using control myocytes, we confirmed the relationship between PKD, LPL, and caspase-3. Thus, the phosphomimetic PKD colocalized with LPL in the trans-golgi, facilitating LPL secretion to cardiomyocyte cell surface. In addition, PKD mutated to prevent its cleavage by caspase-3 or silencing of caspase-3 was able to increase LPL activity. Overall, our data suggest that caspase-3, by cleaving PKD, limits LPL vesicle formation and eventual increase of LPL at the vascular lumen.

Z-DEVD-fmk is a potent, irreversible, and cell-permeable inhibitor of caspase-3. Using this compound in D-100
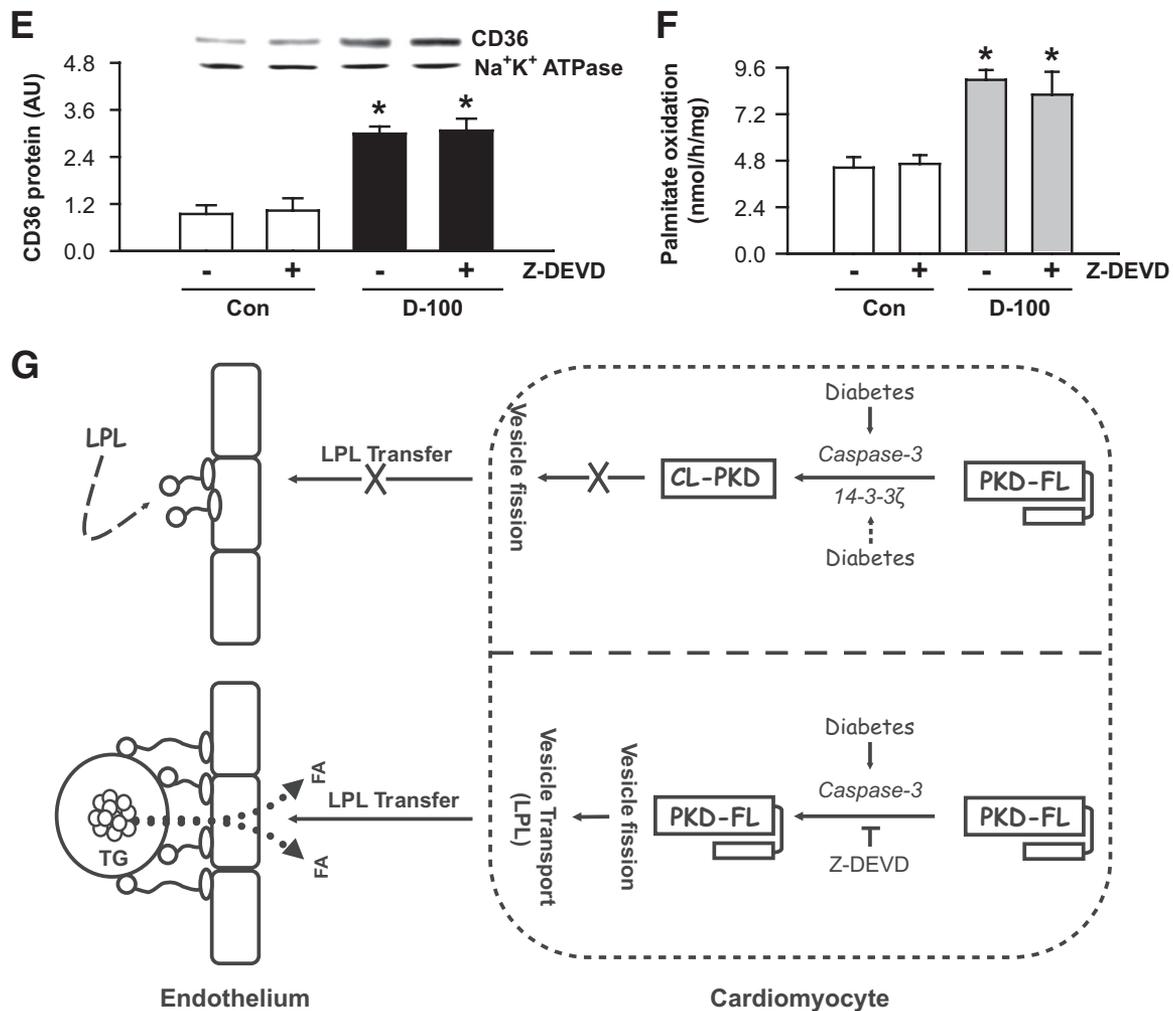
FIG. 7. Continued.

animals, we effectively lowered caspase-3 activity, prevented PKD cleavage, and increased LPL vesicle formation and translocation to the vascular lumen. This increase in LPL at the vascular lumen occurred even though the total LPL protein expression remained ~20% lower than that in control subjects. It should be noted that electron microscopy using immunogold labeling established that in the heart, 78% of total LPL is present in cardiac myocytes, 3–6% in the interstitial space, and 18% at the coronary endothelium (6). Thus, LPL at the vascular lumen is likely more dependent on the signaling that promotes transfer of this enzyme from the cardiomyocyte to the coronary lumen rather than its absolute cardiomyocyte content.

Cardiac LPL is a major determinant of plasma triglyceride (37). Thus, the increase in cardiac luminal LPL in Z-DEVD–treated D-100 animals could explain the decline in circulating triglyceride. Whether other tissue LPL contributes toward this observed fall in plasma triglyceride is unknown because heparin perfusion to release vascular-bound LPL is difficult to accomplish in other tissues. As no apparent change was noted in plasma fatty acid levels in these animals, our data suggest that following LPL-mediated triglyceride hydrolysis, fatty acids can be taken rapidly and directly into tissues. In support of this suggestion, cardiac- and skeletal muscle–specific overexpression of LPL decreased plasma triglyceride and elevated triglyceride storage in muscle tissue but was without effect when

plasma fatty acid was measured (38). In the event of an increased availability of fatty acid, its disposal can occur either via oxidation or via its conversion into triglyceride, which serves as the primary storage form of fatty acids. Caspase-3 inhibition did not alter the high fatty acid uptake and oxidation in D-100 rats. However, measurement and visualization of cardiac triglyceride revealed a striking accumulation in Z-DEVD–treated D-100 hearts, which was almost twofold higher than that in the untreated D-100 animals. This triglyceride was richly associated with the lipid-storage droplet protein, OXPAT (39). Overall, these data suggest that in D-100 hearts treated with Z-DEVD, fatty acid uptake and oxidation are likely operating at their maximum capacity. The additional triglyceride accumulation in this group is most likely a consequence of an increase in LPL and vascular lipolysis, with the released fatty acids rapidly taken up and stored as triglycerides with the assistance of OXPAT. Other studies have also reported excessive triglyceride overload when LPL is specifically overexpressed in the heart (40). It should be recognized that PKD has also been linked to GLUT4-mediated glucose uptake in contracting myocytes (41). However, as STZ diabetes rapidly decreases the myocardial content of total membrane GLUT4 ($t_{1/2}$ of 3.5 days) (42), the impact of PKD in regulating glucose uptake is likely minimal under conditions of hypoinsulinemia and hyperglycemia.

In summary, severe hypoinsulinemia with its associated increase in circulating fatty acids and triglycerides lowers 14-3-3ζ expression and activates caspase-3, which can cleave PKD, reduce LPL vesicle fission, and restrict LPL translocation to the vascular lumen (Fig. 7*G*). When caspase-3 is inhibited, this compensatory response is lost, leading to accumulation of triglycerides (Fig. 7*G*). It should be noted that in transgenic rabbits that have global overexpression of LPL, attenuation of hypertriglyceridemia was observed, an effect suggested to contribute toward amelioration of insulin resistance and obesity (43). Contrary to systemic overexpression, tissue-specific overexpression of LPL in skeletal muscle and heart is associated with lipid oversupply, insulin resistance, and severe myopathy, characterized by muscle fiber degeneration, extensive proliferation of mitochondria and peroxisomes, excessive dilatation, and impaired left ventricular systolic function (18,38,40,44,45). Interestingly, drugs such as pioglitazone that are known to decrease caspase-3 (46) have been reported to reduce circulating triglycerides (47,48) by increasing LPL in humans (49) and to increase the myocardial content of lipids in rats fed a high-fat diet (50). Whether this effect can explain the risk of heart failure when thiazolidenediones are used in patients with type 2 diabetes has yet to be determined (51,52). Thus, although caspase inhibition has been considered to have therapeutic effects in many human diseases, including heart attack, neurodegenerative diseases, and autoimmune disorders, its use in diabetes to prevent cardiac cell death could lead to significant cardiac triglyceride accumulation and warrants further investigation.

ACKNOWLEDGMENTS

REFERENCES

1. Avogaro A, Nosadini R, Doria A, Fioretto P, Velussi M, Vigorito C, Sacca L, Toffolo G, Cobelli C, Trevisan R, et al. Myocardial metabolism in insulin-deficient diabetic humans without coronary artery disease. Am J Physiol 1990;258:E606–E618
2. Saddik M, Lopaschuk GD. Myocardial triglyceride turnover and contribution to energy substrate utilization in isolated working rat hearts. J Biol Chem 1991;266:8162–8170
3. Lopaschuk GD, Belke DD, Gamble J, Itoi T, Schonekess BO. Regulation of fatty acid oxidation in the mammalian heart in health and disease. Biochim Biophys Acta 1994;1213:263–276
4. Paulson DJ, Crass MF 3rd. Endogenous triacylglycerol metabolism in diabetic heart. Am J Physiol 1982;242:H1084–H1094
5. Haffner SM. Lipoprotein disorders associated with type 2 diabetes mellitus and insulin resistance. Am J Cardiol 2002;90:55i–61i
6. Blanchette-Mackie EJ, Masuno H, Dwyer NK, Olivecrona T, Scow RO. Lipoprotein lipase in myocytes and capillary endothelium of heart: immunocytochemical study. Am J Physiol 1989;256:E818–E828
7. Merkel M, Eckel RH, Goldberg IJ. Lipoprotein lipase: genetics, lipid uptake, and regulation. J Lipid Res 2002;43:1997–2006
8. Augustus AS, Kako Y, Yagyu H, Goldberg IJ. Routes of FA delivery to cardiac muscle: modulation of lipoprotein lipolysis alters uptake of TG-derived FA. Am J Physiol Endocrinol Metab 2003;284:E331–E339
9. Camps L, Reina M, Llobera M, Vilaro S, Olivecrona T. Lipoprotein lipase: cellular origin and functional distribution. Am J Physiol 1990;258:C673–C681
10. Eckel RH. Lipoprotein lipase. A multifunctional enzyme relevant to common metabolic diseases. N Engl J Med 1989;320:1060–1068
11. Blanchette-Mackie EJ, Dwyer NK, Amende LA. Cytochemical studies of lipid metabolism: immunogold probes for lipoprotein lipase and cholesterol. Am J Anat 1989;185:255–263
12. Rodrigues B, Cam MC, McNeill JH. Myocardial substrate metabolism: implications for diabetic cardiomyopathy. J Mol Cell Cardiol 1995;27:169–179
13. Pulinilkunnil T, Abrahani A, Varghese J, Chan N, Tang I, Ghosh S, Kulpa J, Allard M, Brownsey R, Rodrigues B. Evidence for rapid "metabolic switching" through lipoprotein lipase occupation of endothelial-binding sites. J Mol Cell Cardiol 2003;35:1093–1103
14. Rodrigues B, Cam MC, Jian K, Lim F, Sambandam N, Shepherd G. Differential effects of streptozotocin-induced diabetes on cardiac lipoprotein lipase activity. Diabetes 1997;46:1346–1353
15. Pulinilkunnil T, Qi D, Ghosh S, Cheung C, Yip P, Varghese J, Abrahani A, Brownsey R, Rodrigues B. Circulating triglyceride lipolysis facilitates lipoprotein lipase translocation from cardiomyocyte to myocardial endothelial lining. Cardiovasc Res 2003;59:788–797
16. Sambandam N, Abrahani MA, St Pierre E, Al-Atar O, Cam MC, Rodrigues B. Localization of lipoprotein lipase in the diabetic heart: regulation by acute changes in insulin. Arterioscler Thromb Vasc Biol 1999;19:1526–1534
17. Sambandam N, Abrahani MA, Craig S, Al-Atar O, Jeon E, Rodrigues B. Metabolism of VLDL is increased in streptozotocin-induced diabetic rat hearts. Am J Physiol Heart Circ Physiol 2000;278:H1874–H1882
18. Kim MS, Wang F, Puthanveetil P, Kewalramani G, Hosseini-Beheshti E, Ng N, Wang Y, Kumar U, Innis S, Proud CG, Abrahani A, Rodrigues B. Protein kinase D is a key regulator of cardiomyocyte lipoprotein lipase secretion after diabetes. Circ Res 2008;103:252–260
19. An D, Pulinilkunnil T, Qi D, Ghosh S, Abrahani A, Rodrigues B. The metabolic "switch" AMPK regulates cardiac heparin-releasable lipoprotein lipase. Am J Physiol Endocrinol Metab 2005;288:E246–E253
20. Kim MS, Kewalramani G, Puthanveetil P, Lee V, Kumar U, An D, Abrahani A, Rodrigues B. Acute diabetes moderates trafficking of cardiac lipoprotein lipase through p38 mitogen-activated protein kinase-dependent actin cytoskeleton organization. Diabetes 2008;57:64–76
21. Pillarisetti S, Paka L, Sasaki A, Vanni-Reyes T, Yin B, Parthasarathy N, Wagner WD, Goldberg IJ. Endothelial cell heparanase modulation of lipoprotein lipase activity. Evidence that heparan sulfate oligosaccharide is an extracellular chaperone. J Biol Chem 1997;272:15753–15759
22. Wang F, Kim MS, Puthanveetil P, Kewalramani G, Deppe S, Ghosh S, Abrahani A, Rodrigues B. Endothelial heparanase secretion after acute hypoinsulinemia is regulated by glucose and fatty acid. Am J Physiol Heart Circ Physiol 2009;296:H1108–H1116
23. Junod A, Lambert AE, Stauffacher W, Renold AE. Diabetogenic action of streptozotocin: relationship of dose to metabolic response. J Clin Invest 1969;48:2129–2139
24. Kewalramani G, An D, Kim MS, Ghosh S, Qi D, Abrahani A, Pulinilkunnil T, Sharma V, Wambolt RB, Allard MF, Innis SM, Rodrigues B. AMPK control of myocardial fatty acid metabolism fluctuates with the intensity of insulin-deficient diabetes. J Mol Cell Cardiol 2007;42:333–342
25. Braun JE, Severson DL. Diabetes reduces heparin- and phospholipase C-releasable lipoprotein lipase from cardiomyocytes. Am J Physiol 1991;260:E477–E485
26. Endo K, Oki E, Biedermann V, Kojima H, Yoshida K, Johannes FJ, Kufe D, Datta R. Proteolytic cleavage and activation of protein kinase C [micro] by caspase-3 in the apoptotic response of cells to 1-β-D-arabinofuranosylcytosine and other genotoxic agents. J Biol Chem 2000;275:18476–18481
27. Maeda Y, Beznoussenko GV, Van Lint J, Mironov AA, Malhotra V. Recruitment of protein kinase D to the trans-Golgi network via the first cysteine-rich domain. Embo J 2001;20:5982–5990
28. Tzivion G, Avruch J. 14–3-3 proteins: active cofactors in cellular regulation by serine/threonine phosphorylation. J Biol Chem 2002;277:3061–3064
29. Kim YH, Kim YS, Kang SS, Noh HS, Kim HJ, Cho GJ, Choi WS. Expression of 14–3-3 zeta and interaction with protein kinase C in the rat retina in early diabetes. Diabetologia 2005;48:1411–1415
30. Matthews SA, Rozengurt E, Cantrell D. Characterization of Ser^916 as an in vivo autophosphorylation site for protein kinase D/Protein kinase Cmu. J Biol Chem 1999;274:26543–26549
31. Matthews SA, Pettit GR, Rozengurt E. Bryostatin 1 induces biphasic activation of protein kinase D in intact cells. J Biol Chem 1997;272:20245–20250
32. Lu G, Chen J, Espinoza LA, Garfield S, Toshiyuki S, Akiko H, Huppler A, Wang QJ. Protein kinase D 3 is localized in vesicular structures and

interacts with vesicle-associated membrane protein 2. Cell Signal 2007;19: 867–879

33. An D, Rodrigues B. Role of changes in cardiac metabolism in development of diabetic cardiomyopathy. Am J Physiol Heart Circ Physiol 2006;291: H1489–H1506

34. Cai L, Li W, Wang G, Guo L, Jiang Y, Kang YJ. Hyperglycemia-induced apoptosis in mouse myocardium: mitochondrial cytochrome C-mediated caspase-3 activation pathway. Diabetes 2002;51:1938–1948

35. Porter AG, Janicke RU. Emerging roles of caspase-3 in apoptosis. Cell Death Differ 1999;6:99–104

36. Kuranaga E, Miura M. Nonapoptotic functions of caspases: caspases as regulatory molecules for immunity and cell-fate determination. Trends Cell Biol 2007;17:135–144

37. Levak-Frank S, Hofmann W, Weinstock PH, Radner H, Sattler W, Breslow JL, Zechner R. Induced mutant mouse lines that express lipoprotein lipase in cardiac muscle, but not in skeletal muscle and adipose tissue, have normal plasma triglyceride and high-density lipoprotein-cholesterol levels. Proc Natl Acad Sci U S A 1999;96:3165–3170

38. Levak-Frank S, Radner H, Walsh A, Stollberger R, Knipping G, Hoefler G, Sattler W, Weinstock PH, Breslow JL, Zechner R. Muscle-specific overexpression of lipoprotein lipase causes a severe myopathy characterized by proliferation of mitochondria and peroxisomes in transgenic mice. J Clin Invest 1995;96:976–986

39. Wolins NE, Quaynor BK, Skinner JR, Tzekov A, Croce MA, Gropler MC, Varma V, Yao-Borengasser A, Rasouli N, Kern PA, Finck BN, Bickel PE. OXPAT/PAT-1 is a PPAR-induced lipid droplet protein that promotes fatty acid utilization. Diabetes 2006;55:3418–3428

40. Yagyu H, Chen G, Yokoyama M, Hirata K, Augustus A, Kako Y, Seo T, Hu Y, Lutz EP, Merkel M, Bensadoun A, Homma S, Goldberg IJ. Lipoprotein lipase (LPL) on the surface of cardiomyocytes increases lipid uptake and produces a cardiomyopathy. J Clin Invest 2003;111:419–426

41. Luiken JJ, Vertommen D, Coort SL, Habets DD, El Hasnaoui M, Pelsers MM, Viollet B, Bonen A, Hue L, Rider MH, Glatz JF. Identification of protein kinase D as a novel contraction-activated kinase linked to GLUT4-mediated glucose uptake, independent of AMPK. Cell Signal 2008;20:543–556

42. Garvey WT, Hardin D, Juhaszova M, Dominguez JH. Effects of diabetes on myocardial glucose transport system in rats: implications for diabetic cardiomyopathy. Am J Physiol 1993;264:H837–H844

43. Kitajima S, Morimoto M, Liu E, Koike T, Higaki Y, Taura Y, Mamba K, Itamoto K, Watanabe T, Tsutsumi K, Yamada N, Fan J. Overexpression of lipoprotein lipase improves insulin resistance induced by a high-fat diet in transgenic rabbits. Diabetologia 2004;47:1202–1209

44. Kim JK, Fillmore JJ, Chen Y, Moore IK, Pypaert M, Lutz EP, Kako Y, Velez-Carrasco W, Goldberg IJ, Breslow JL, Shulman GI. Tissue-specific overexpression of lipoprotein lipase causes tissue-specific insulin resistance. Proc Natl Acad Sci U S A 2001;98:7522–7527

45. Wang H, Knaub LA, Jensen DR, Young Jung D, Hong EG, Ko HJ, Coates AM, Goldberg IJ, de la Houssaye BA, Janssen RC, McCurdy CE, Rahman SM, Soo Choi C, Shulman GI, Kim JK, Friedman JE, Eckel RH. Skeletal muscle-specific deletion of lipoprotein lipase enhances insulin signaling in skeletal muscle but causes insulin resistance in liver and other tissues. Diabetes 2009;58:116–124

46. Li J, Lang MJ, Mao XB, Tian L, Feng YB. Antiapoptosis and mitochondrial effect of pioglitazone preconditioning in the ischemic/reperfused heart of rat. Cardiovasc Drugs Ther 2008;22:283–291

47. Boyle PJ, King AB, Olansky L, Marchetti A, Lau H, Magar R, Martin J. Effects of pioglitazone and rosiglitazone on blood lipid levels and glycemic control in patients with type 2 diabetes mellitus: a retrospective review of randomly selected medical records. Clin Ther 2002;24:378–396

48. Kobayashi J, Nagashima I, Hikita M, Bujo H, Takahashi K, Otabe M, Morisaki N, Saito Y. Effect of troglitazone on plasma lipid metabolism and lipoprotein lipase. Br J Clin Pharmacol 1999;47:433–439

49. Nagashima K, Lopez C, Donovan D, Ngai C, Fontanez N, Bensadoun A, Fruchart-Najib J, Holleran S, Cohn JS, Ramakrishnan R, Ginsberg HN. Effects of the PPAR-γ agonist pioglitazone on lipoprotein metabolism in patients with type 2 diabetes mellitus. J Clin Invest 2005;115:1323–1332

50. Baranowski M, Blachnio-Zabielska A, Zabielski P, Gorski J. Pioglitazone induces lipid accumulation in the rat heart despite concomitant reduction in plasma free fatty acid availability. Arch Biochem Biophys 2008;477:86–91

51. Lago RM, Singh PP, Nesto RW. Congestive heart failure and cardiovascular death in patients with prediabetes and type 2 diabetes given thiazolidinediones: a meta-analysis of randomised clinical trials. Lancet 2007;370:1129–1136

52. Lipscombe LL, Gomes T, Levesque LE, Hux JE, Juurlink DN, Alter DA. Thiazolidinediones and cardiovascular outcomes in older patients with diabetes. JAMA 2007;298:2634–2643